Environ. Sci. Technol. **2004**, *38,* 4878−4883

Removal of Industrial Cutting Oil from Oil Emulsions by Polymeric Ultra- and Microfiltration Membranes

PETER JANKNECHT, ANA D. LOPES, AND ADÉLIO M. MENDES*

Chemical Engineering Department, Faculty of Engineering, University of Porto, Rua Dr. Roberto Frias, 4200-465 Porto, Portugal

The utilization of micro- and ultrafiltration with polymeric membranes for treatment of industrial cutting oil emulsion was investigated. The performance of 14 different membranes with pore sizes in the range of 1−800 nm, representing 8 different materials and varying hydrophobicity, was determined experimentally. Membrane permeances between 1.6 and 939 L m^{-2} h^{-1} bar^{-1} have been observed for the different samples as well as oil rejections between 3.42% and 99.99%. Membrane pore size and contact angle showed little influence on both values, while an interesting correlation is displayed to the individual membranes' capillary pressures. A possible explanation for this phenomenon is suggested based on the formation of oil films on the membrane surface. From the investigated membranes, the best-suited one for cutting oil treatment was selected and subjected to further experiments. The effect of process temperatures between 22 and 43 °C and of feed oil concentrations between 0 and 20 vol % on the removal performance was determined. The results correspond to the explanation suggested previously.

Introduction

Emulsions are two-phase mixtures of microscopic oil droplets in an aqueous solution and are technically utilized in numerous machining processes. Emulsions containing 3−10 vol % of mineral oil in water are commonly employed in metal cutting processes such as drilling, milling, turning, or grinding. They serve several purposes including lubrication, cooling of tools and machined surfaces, removal of metal particles from the cutting edges, and inhibition of corrosion.

To stabilize such emulsion systems, surfactants are usually added to the mixture. They considerably reduce the surface tension so that microscopic oil droplets can be formed, which are continuously kept in dispersion by Brownian molecular movements. Thus flotation of the droplets and subsequent separation of the phases is avoided, and the emulsion remains stable.

Emulsions utilized in machining processes are usually recovered, cooled, and—after particle removal by sedimentation and/or filtration—recycled. The alternating exposure to high temperature and pressure changes, however, leads to a continuous degeneration of the hydrocarbon compounds, so that the emulsion ultimately must be discharged.

* Corresponding author phone: +351 225 081 695; e-mail: mendes@fe.up.pt.

The main environmental risk associated with this discharge is the mineral oil portion of the emulsion, which is usually recalcitrant to biological degradation and threatens the biological activity in natural water bodies (*1*). Strict limits for the oil content of discharged wastewater are therefore set up, both for direct and indirect discharge. The Portuguese law DL 232/99 sets the limit for oil content in residual wastewater at 15 mg L^{-1}.

Therefore, it is necessary to reliably remove the oil portion of the emulsion at the point of discharge after its normal life span, enabling separate and simple treatment of the two individual phases. This treatment step is conventionally accomplished by chemical treatment and flotation or sedimentation (*1*, *2*), by evaporation (*3*), or by ultrafiltration with ceramic membranes (*4*−*6*). So far, little information exists in published literature about the utilization of polymeric membranes, which due to their comparatively low price represent an attractive approach to this field:

(i) Karakulski and Morawski (*7*) studied the application of different ultrafiltration membranes made of PVDF, PVC, and PAN for the treatment of spent copper wire drawing emulsion, but only as a pretreatment for subsequent reverse osmosis by spiral-wound Filmtec BW3040 membrane elements.

(ii) Chang et al. (*8*) employed an UF pilot plant to treat degreasing and cutting oil wastewater generated from the automobile components industry, finding the performance of the filtration process with the cutting oil emulsion so poor that only pretreatment with ozone allowed the reuse of the UF permeates as process water.

(iii) Benito et al. (*9*) optimized the operating conditions for ultrafiltration of a synthetic cutting oil emulsion with four organic membranes made of polysulfone and regenerated cellulose, respectively.

The subject of this work was to study the performance of 14 different membranes, representing 8 different materials with varying hydrophobicity and pore sizes in the range of 1−800 nm. Subsequently, the effect of different operating temperatures and feed oil concentrations on the filtration performance of the best suited of these membranes was studied.

Experimental Section

Seven microfiltration and seven ultrafiltration membranes were utilized in the comparative experiments. By convention, the pore diameter (D_p) for a microfiltration membrane is quoted in micrometers (μm) while for ultrafiltration membranes it is common to relate to the molecular weight cutoff (MWCO) expressed as atomic units (au). Within this study, for reasons of better comparability and in order to approximate the membranes' capillary pressure, the cutoff weight is transformed into nanometers (nm) of pore diameter by the following equation derived from literature values (*4*):

$$D_p \approx 10^{-4}\ \text{nm} \times \left(\frac{\text{MWCO}}{\text{au}}\right) \quad (1)$$

Pore diameters of all membranes in this study ranged from 0.1 to 800 nm. The individual membranes' characteristics are listed in Table 1.

All membranes were investigated as flat sheet samples, sized 191 by 140 mm and mounted in an OSMONICS SEPA CF module with 155 cm^2 effective membrane area. The flow scheme of the experimental setup is depicted in Figure 1. The oil emulsion utilized in the experiments was prepared from distilled water with the industrial metal working oil

10.1021/es0348243 CCC: $27.50
Published on Web 08/06/2004

TABLE 1. Characteristics of the Studied Membranes

Ultrafiltration Membranes

membrane	manufacturer	material	MWCO (au)	D_p (nm)	max recom pressure (bar)
HG 26	Osmonics	polysulfone	1−5000	0.1−0.5[a]	7.0
AG 08	Osmonics	fluorpolymer	1−15 000	0.1−1.5[a]	5.0
HN 30	Osmonics	polysulfone	15−25 000	1.5−2.5[a]	3.5
SN 32	Osmonics	cellulose	15−30 000	1.5−3.0[a]	3.5
PAN HV4	GKSS	polyacrylonitrile	30 000	3.0	2.0
RZ 04	Osmonics	acryl	40−60 000	4.0−6.0[a]	2.0
HZ 20	Osmonics	polysulfone	40−60 000	4.0−6.0[a]	2.0

Microfiltration Membranes

membrane	manufacturer	material	D_p (μm)	D_p (nm)	max recom pressure (bar)
YL 01	Osmonics	polypropylene	0.02	20	2.0
YB 01	Osmonics	polypropylene	0.04	40	2.0
YK 01	Osmonics	polypropylene	0.10	100	2.0
WC 02	Osmonics	(not published)	0.20	200	1.7
MC 04	Osmonics	polyamide	0.20	200	1.7
nylon	Plastok	nylon	0.22	220	2.0
RH 02	Osmonics	acryl	0.80	800	2.0

[a] In the subsequent sections, the pore diameter D_p for the ultrafiltration membranes will be considered the mean value of these limits.

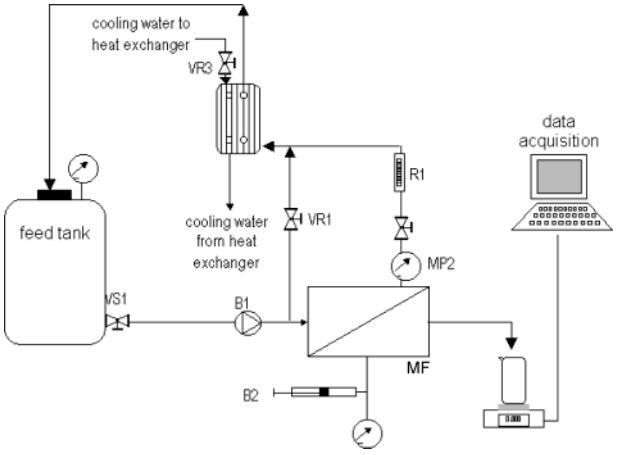

FIGURE 1. Flow scheme of the experimental setup. VS1, tank valve; B1, feed pump; VR1, regulation valve for feed bypass; MF, flat plane membrane filtration module; B2, hand-operated hydraulic pump for closing the module; MP2, pressure gauge for retentate; R1, rotameter for retentate; VR3, regulation valve for cooling water to heat exchanger.

"SECO" by Sun Oil Company (Belgium) N. V., which consists of 85% mineral naphthenic oil and 15% of an anionic surfactant type additive (emulgator). The density of the oil is 981 g L^{-1}. The regular oil content of the emulsion in the experiments was 5% per volume, which corresponds to the manufacturer's recommendation. For some explicitly designated experiments, however, the volume concentration also was varied between 0.5 and 20 volume percent.

For the expected separation by micro- and ultrafiltration, the size of the emulsion's oil droplets was of particular interest. Regretfully, it was not possible to reproducibly determine the size distribution by Laser Diffraction Particle Size Analysis (Malvern Instruments Ltd.), probably due to oil film formation on the optical parts. However, the medium droplet diameter in a 5% emulsion sample could be determined to be in the order of 160 nm by that method.

Oil concentrations during the experiments were measured by a photometrical method. Using a Philips PU 8625 UV/VIS Spectrophotometer the light absorbance in several samples of the utilized kind of emulsion was determined at different wavelengths, yielding a maximum absorption at 734 nm. For

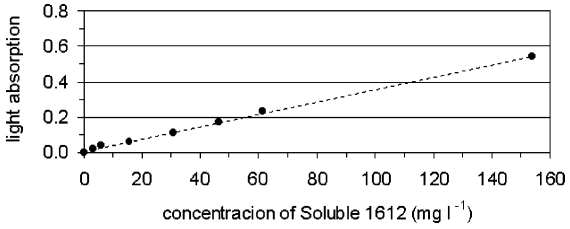

FIGURE 2. Calibration curve for a "soluble 1612" emulsion in water.

that wavelength, a calibration curve was generated using a 20 vol % stock emulsion and 6 successive dilution steps. Individual samples analyzed by the gravimetric extraction method designated 5520 B in the "Standard Methods for the Examination of Water and Wastewater" confirmed the results obtained with this method, which are depicted in Figure 2.

The individual experiments were conducted as follows: 10 L of stabilized "soluble 1612" oil emulsion were mixed at the required concentration, homogenized, and filled into the reservoir. A sample was taken for subsequent analysis.

After assembling and closing of the membrane module, the feed side was rinsed, and the cooling water for the heat exchanger was turned on. The permeate outlet was connected to a collector vessel mounted on an electronic balance, which continuously recorded the weight change. Finally the feed pump was activated, and the process conditions were adjusted by two valves in the retentate line and the bypass, which controlled feed flow and pressure, respectively. For the comparative experiments, the feed temperature was adjusted by regulating the cooling water flow through the heat exchanger. For each membrane, the transmembrane pressure was adjusted to the maximum value individually recommended by the manufacturer; otherwise experimental conditions were identical: The temperature was adjusted to 22 °C; oil content of the emulsion was 5 vol %, corresponding to 38 g L^{-1}; and the feed flow was 3 L min^{-1}, resulting in a tangential flow velocity across the membrane surface of 0.33 m s^{-1}.

The permeate flow reached steady state within a period of about 5−10 min, then the flow was recorded and a sample was taken. Both the feed and permeate samples were analyzed for oil content. After each experiment, the membrane was washed and the permeance was subsequently checked with distilled water. No decrease over time was determined.

TABLE 2. Results of Filtration Experiments and Contact Angle Measurements with Different Membranes

membrane	material	D_p (nm)	pressure (bar)	permeance (L m^{-2} h^{-1} bar^{-1})	permeate oil concn (mg L^{-1})	oil rejection (%)	contact angle (deg)	capillary pressure (bar)
HG 26	polysulfone	0.3	7	1.6	2.2	99.99	71	−3.1
AG 08	fluorpolymer	0.8	5	9	2.3	99.99	81	−0.57
HN 30	polysulfone	2.0	3.5	16	2.4	99.99	80	−0.25
SN 32	cellulose	2.3	3.5	1.9	3.9	99.99	58	−0.68
PAN HV3	polyacrylonitrile	3.0	2	2.2	6.2	99.98		
RZ 04	acryl	5.0	2	39	5.4	99.98	85	−0.05
HZ 20	polysulfone	5.0	2	4.9	2.2	99.99	80	−0.10
YL 01	polypropylene	20	2	0			105	0.037
YB 01	polypropylene	40	2	0			116	0.032
YK 01	polypropylene	100	2	10	350	99.08	100	0.005
WC 02	unknown	200	1.7	19	35500	6.58	92	0.0005
MC 04	polyamide	200	1.7	46	2233	94.12	98	0.002
Nylon	nylon	220	2	939	36700	3.42	77	−0.003
RH 02	acryl	800	2	147	25100	33.95	100	0.0006

Contact angle measurements of the individual membranes were conducted using a Dataphysics "OCA 15 plus" measurement system. The values were determined by computerized image analysis using the Laplace−Young method.

Results and Discussion

The practical work of this study was conducted in two successive steps. In the first step the permeance and rejection rate of the polymeric micro- and ultrafiltration membranes with oil emulsion were determined. The oil rejection rate was calculated by dividing the permeate concentration by the feed concentration, and it corresponds to the portion of the oil content that is held back by the membrane. These experiments were carried out with fresh emulsion and for interesting cases confirmed with real waste emulsion from a metal machining factory. In the second step, the best-suited membrane for the treatment process was selected, and the effect of different operating parameters on the separation performance was studied.

Permeance and Rejection of Different Membranes. In the first part of this study, each membrane was tested under identical experimental conditions and in the experimental setup described earlier. The results are listed in Table 2.

Among the investigated ultrafiltration membranes, none displayed a rejection rate of less than 99.98%, while literature values for practical applications are in the order of only 97% (*5*). For the microfiltration membranes, however, rejection values varied widely between 99.08% (YK 01) and 3.42% (Nylon 0.22 μm).

While in these experiments some rough trend could be observed between increasing membrane pore size and permeate oil content, no correlation was apparent between pore size and permeance. In fact, the two membranes YB01 and YK01 proved to be practically impenetrable by the emulsion despite of their comparatively large pore size of 40 and 100 nm, respectively.

The peculiar behavior of these membranes is likely to be caused by their surface properties, since both in subsequent measurements turned out to be very hydrophobic. Hydrophobicity is commonly quantified as the contact angle of a water−air interface with the respective solid material. Contact angles above 90° indicate a hydrophobic surface, and those below 90° indicate a hydrophilic one. The hydrophobicity of the material largely influences capillary effects that occur inside the pores of micro- or ultrafiltration membranes and affect the permeate flow or rejection of a liquid. Though an air−water interface does not represent the conditions encountered in the filtration of an oil emulsion, it can be a useful model due to the fact that hydrophobicity and oleophilicity are both coupled to the same molecular features and generally occur together.

To obtain the contact angles, measurements with the different membranes were carried out after the experimental runs. This is essential because previous work has demonstrated that during microfiltration of emulsions the removed oil phase tends to adsorb to the membrane surface, thus considerably changing the membrane's effective surface behavior (*10*, *11*).

No direct correlation was observed between the membranes' contact angles and their flux or oil rejection, which was to be expected since the contact angle is but one parameter involved in capillary effects. To quantify these, the capillary pressure (p_C) can be calculated from the contact angle (θ), surface tension of water (γ), and pore diameter (D_p) according to the following equation given by Baer (*12*):

$$p_c = \frac{4\gamma \cos \theta}{D_p} \tag{2}$$

The capillary pressure is the overpressure needed for the air to drive water out of a given capillary or pore. As apparent from eq 2, for hydrophobic surfaces with contact angles $\theta > 90°$, the capillary pressure becomes negative. In this case the surface is not wetted by the water and expels it from the pores even without air over pressure. From the measured contact angles, the capillary pressure for each membrane was calculated according to eq 2, based on the known pore diameters of the individual membranes and the literature value for the surface tension of 72 m N m^{-1} between air and water.

It has to be pointed out that the results of this calculation listed in the right columns of Table 2 do not correspond to the physical conditions during filtration since both contact angle and surface tension here are for water in contact with air instead of oil. The authors propose the utilization of the capillary pressure with air instead of oil because its value is characteristic for every membrane and independent of the oil phase and surfactants with which the measurements are carried out. Both oil composition and surfactant content strongly affect contact angles so that the capillary pressure with oil would have to be determined for every application individually. Yet its practical validity would remain doubtful since possible contamination during operation still can change its value considerably.

Thus the capillary pressure of the water−membrane−air system, though theoretically less precise, might prove a more useful tool for the description of different membranes' suitability for the filtration of oil emulsions. Since hydrophilicity and oleophobicity are coupled with the underlying molecular polarity, these values constitute a good model and give a qualitative understanding of the surface interactions and their effects on membrane performance.

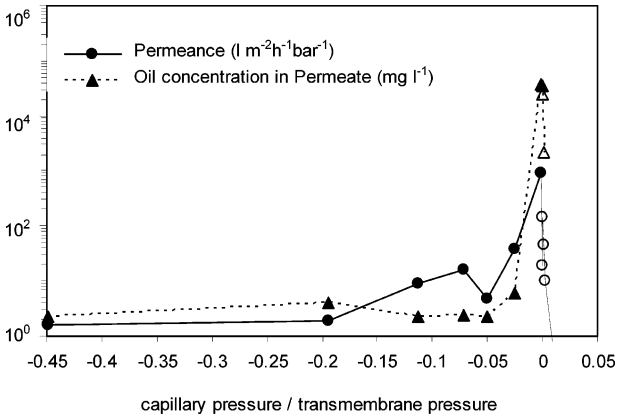

FIGURE 3. Permeance and oil content correlated to pressure ratio. Solid symbols represent ultrafiltration membranes; open symbols represent microfiltration membranes. Individual data points correspond to the following membranes (left to right): HG 26, SN 32, AG 08, HN 30, HZ 20, RZ 04, nylon, WC 02, RH 02, MC 04, and YK 01 The points for YB 01 and YL 01 are on the right end of the curves out of the diagram.

It is also important to point out that classical contact angle measurement with a smooth dense material yields different results than with a porous membrane. Yet, the goal of the measurements in this case is not so much to determine the surface energy of the pure membrane material but to practically characterize porous membranes with respect to the filtration of oil suspensions. This characterization can actually be improved by including possible pore effects in the contact angle measurements, as these can be expected to reflect corresponding effects in the filtration process and thus (in this particular application) increase the validity of the results. This is in fact supported by the results displayed in Figure 3, where the ratio of calculated capillary pressure (with air) versus transmembrane pressure applied in the filtration is related to the observed permeance and oil rejection.

Considering the fact that a wide range of membranes from different materials and with correspondingly heterogeneous morphology and pore structure are directly compared, the obvious correlation in this diagram is extremely interesting. It indicates that for this liquid two-phase system neither pore size nor contact angle alone determine the flux and rejection behavior, but their interaction represented here by the capillary pressure.

The diagram yields a clear correlation, in that both the highest bulk flux and the highest permeate oil content occur at zero capillary pressure. Both parameters drop rapidly at increasingly positive capillary pressure (right side, hydrophilic membranes) whereas the drop for negative capillary pressure (left side, hydrophobic membranes) occurs slower for both parameters.

This phenomenon appears to be correlated to the formation of a layer of oil along the membrane surface and pore walls, which also has been observed by other authors and increases both the oil rejection rate and the flow resistance (*10*, *13*).

Two different effects can be assumed to cause this phenomenon. On hydrophobic/oleophilic membrane surfaces (represented by negative pressure ratio on the diagram's left side) the oil droplets are attracted and adsorbed. Even with stabilizing surfactants the free energy at the oil−water interface remains positive, so that the droplets tend to coalesce and form a continuous oil layer directly on the oleophilic membrane and pore surface (Figure 4a).

Hydrophilic/oleophobic membranes (positive pressure ratio), however, reject oil and attract water, thus maintaining a layer of adsorbed water between their surface and the accumulating oil. In this case, depending on the hydrodynamic conditions, the oil droplets may either accumulate above that water layer during filtration, ultimately forming a gel (Figure 4c), or they rupture and yield a continuous oil layer (Figure 4d). Both effects increase the flow resistance and oil rejection of the membrane considerably and lead to the decrease of flux and rejection when the capillary pressure (and thus the pressure ratio) becomes much higher or lower than zero. The slower flux decrease for negative pressure ratio may be explained by the fact that oil directly adsorbed on hydrophobic/olephilic membranes forms a thinner layer and thus affects the filtration less than the floating oil or gel layer on hydrophilic/oleophobic membranes.

Membranes with neutral surface behavior (Figure 4b, pressure ratio around zero) neither attract nor reject the oil droplets. Thus, none of the effects described above occurs and both phases pass through the membrane relatively unobstructed, resulting in high flux and low rejection rate as was observed in the experiments.

Selection and Testing of Best-Suited Membrane. The oil removal performance of all ultrafiltration membranes tested in this study exceeded the requirements set by Portuguese law DL 232/99 for oil content of 15 mg L^{-1} in residual wastewater. The obtainable flux, however, differed consider-

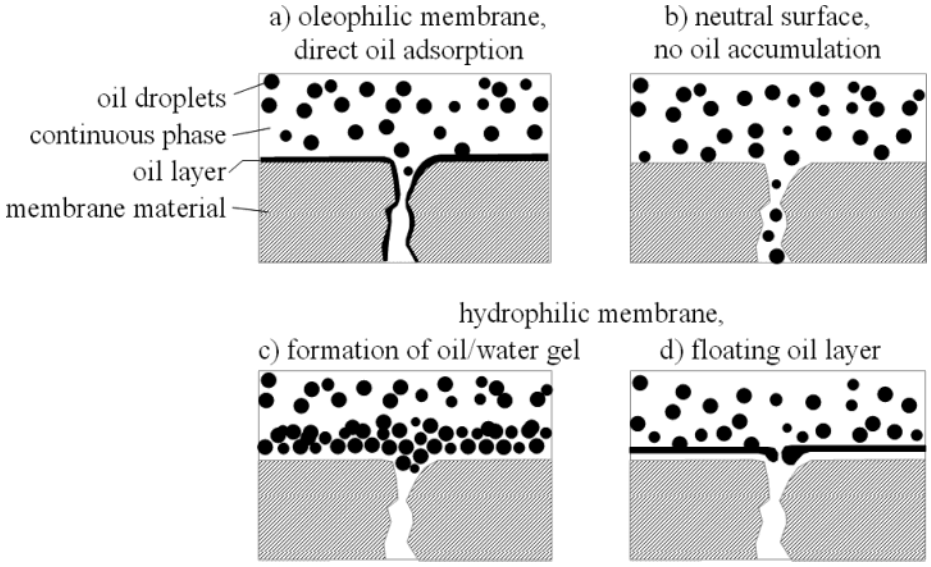

FIGURE 4. Filtration with hydrophobic (a), neutral (b), and hydrophilic (c, d) membrane.

TABLE 3. Results Obtained with Model Emulsion and Real Effluent Emulsion at 22 °C

membrane	pressure (bar)	feed oil concn ($g\ L^{-1}$) model emulsion	feed oil concn ($g\ L^{-1}$) real effluent	permeate oil concn ($mg\ L^{-1}$) model emulsion	permeate oil concn ($mg\ L^{-1}$) real effluent	permeance ($L\ m^{-2}\ h^{-1}\ bar^{-1}$) model emulsion	permeance ($L\ m^{-2}\ h^{-1}\ bar^{-1}$) real effluent
AG 08	5.0	38.5	30.2	2.3	2.5	9	8
HN 30	3.5	38.5	30.2	2.4	2.7	16	15
RZ 04	2.0	38.5	30.2	5.4	6.3	39	38

TABLE 4. Effect of Temperature and Feed Oil Concentration on Performance of Membrane RZ 04

feed oil concn (% vol)	temp (°C)	pressure (bar)	tangential flow velocity (ms^{-1})	permeance ($L\ m^{-2}\ h^{-1}\ bar^{-1}$)	permeate oil concn ($mg\ L^{-1}$)	rejection (%)
0.0	22	2	0.33	71	nd[a]	
0.5	22	2	0.33	58	nd	
2.0	22	2	0.33	40	1.6	99.99
5.0	22	2	0.33	37	6.1	99.98
10.0	22	2	0.33	22	8.3	99.99
20.0	22	2	0.33	14	9.5	99.99
0.0	28	2	0.33	170	nd	
0.5	28	2	0.33	75	nd	
2.0	28	2	0.33	50	2.3	99.99
5.0	28	2	0.33	42	6.5	99.98
10.0	28	2	0.33	25	9.1	99.99
20.0	28	2	0.33	15	10.0	99.99
0.0	43	2	0.33	215	nd	
0.5	43	2	0.33	90	nd	
2.0	43	2	0.33	63	3.2	99.98
5.0	43	2	0.33	52	6.7	99.98
10.0	43	2	0.33	30	9.7	99.99
20.0	43	2	0.33	15	12.0	99.99

[a] nd, not detectable.

ably. Since the flux represents an important economical factor in practical membrane applications, only the three membranes with the highest flux were selected for further testing with real effluent from a metal machining process using the same cutting oil as was tested in this study. All experiments were carried out under the standard process parameters described earlier.

The results both with real effluent and with model emulsion are displayed in Table 3. Though the oil concentration in the model emulsion was higher than in the real effluent, the obtained results were similar, which might be explained by the chemical alterations the emulsion undergoes in the machining processes.

The membrane RZ 04 displayed the best flux while performing with an oil rejection rate of 99.99% and therefore was chosen for subsequent investigation. A series of experiments was carried out in which the effects on flux and permeate oil concentration of the parameters temperature, feed oil concentration, pressure, and tangential velocity was to be determined.

Effect of Temperature and Feed Oil Concentration. To assess these parameters, 21 individual experiments were conducted. The results are represented in Table 4.

Figure 5 illustrates the influence of different temperatures and feed oil concentrations on permeance and permeate oil concentration. The concentration range corresponds to the cutting oil manufacturer's recommendations; the selected temperatures are typical for Portuguese metal works.

For higher temperatures in Figure 5a, the permeance increases slightly, which can be contributed to the lower viscosity. Furthermore, for all temperatures a significant decrease of the permeance can be detected for increasing feed oil concentration. While this might be partially caused by the increase of the emulsion's viscosity, it is also in good correspondence with the oil film model proposed earlier since

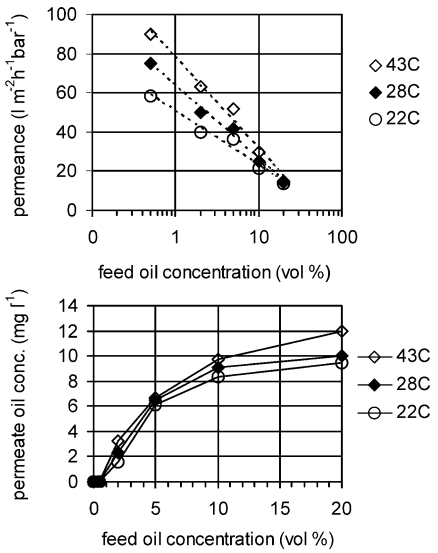

FIGURE 5. Influence of temperature and feed oil concentration on (a) permeance (logarithmic concentration axis) and (b) permeate oil concentration.

the emulsion's oil content must directly affect the oil film's thickness and flow resistance.

In this case the oil film can be regarded as a gel layer, for which the observed logarithmic decrease of flux with increasing feed concentration has been described by other authors (*14*−*16*). According to this literature, the flux is linked to the feed concentration by the following equation:

$$J = k \cdot \ln \frac{C_{gel}}{C_b} \qquad (3)$$

In which J is the "limiting" flux at steady state, C_b is the feed (or bulk) concentration, k is a constant, and C_{gel} is the concentration of the gel layer, which also is considered constant. The correlation described by this equation corresponds to the shape of the curves in Figure 5a.

The correlation between oil concentrations in the feed and permeate depicted in Figure 5b can be contributed to the small portion of the oil that is usually molecularly dissolved within the aqueous phase and cannot be removed by filtration. Both at higher temperatures and higher feed oil concentrations the equilibrium is shifted toward higher dissolved concentrations, thus causing the behavior observed in Figure 5b. This is supported by the fact that at least 99.98% of the oil portion was removed during all these experiments, which indicates the continuous integrity of the process.

Acknowledgments

We appreciate the fruitful discussion with Professor Fernão Magalhães and his suggestions for the manuscript as well as the information kindly provided by Mr. Herwig De Landtsheer of Sun Oil Company (Belgium) N.V.

Literature Cited

(1) Metcalf & Eddy. *Wastewater Engineering*; McGraw-Hill: New York, 1991.

(2) Hartinger, L. *Handbook of Effluent Treatment and Recycling for the Metal Finishing Industry*; Redwood Books; Trowbridge, USA, 1994.

(3) Carreño, C. E. L.; Ipiñazar, E. *Tratamiento de Fluidos de Corte Estudio Comparativo de los Diferentes Processos de Reciclaje*; Residuos; 1998; No 37.

(4) Scott, K. *Handbook of Industrial Membranes*; Elsevier Advanced Technology: Dordrecht, The Netherlands, 1995.

(5) Reed, B. E.; Lin, W.; Dunn, C.; Carriere, P.; Roark, G. Treatment of an oil/grease wastewater using ultrafiltration. *Sep. Sci. Technol.* **1997**, *32*, 1493−1511.

(6) Faibish, R. S.; Cohen, Y. Fouling and rejection behavior of ceramic and polymer-modified ceramic membranes for ultrafiltration of oil-in-water emulsions and microemulsions. *Colloids Surf., A* **2001**, *191*, 27−40.

(7) Karakulski, K.; Morawski, W. A. Purification of copper wire drawing emulsion by application of UF and RO. *Desalination* **2000**, *131*, 87−95.

(8) Chang, I. S.; Chungb, C. M.; Hanb, S. H. Treatment of oily wastewater by ultrafiltration and ozone. *Desalination* **2001**, *133*, 225−232.

(9) Benito, J. M.; Ebel, S.; Gutiérrez, B.; Pazos, C.; Coca, J. Ultrafiltration of a waste emulsified cutting oil using organic membranes. *Water, Air, Soil Pollut.* **2001**, *128*, 181−195.

(10) Mueller, J.; Cen, Y.; Davis, R. H. Cross-flow microfiltration of oily water. *J. Membr. Sci.* **1997**, *129*, 227−237.

(11) Lee, S.; Aurelle, Y.; Roques, H. Concentration polarization, membrane fouling and cleaning in ultrafiltration of soluble oil. *J. Membr. Sci.* **1984**, *19* (1), 23−38.

(12) Baer, J. *Dynamics of Fluids in Porous Media*; Dover Publications: New York, 1972.

(13) Marchese, J.; Ochoa, N. A.; Pagliero, C.; Almandoz, C. Pilot-scale ultrafiltration of an emulsified oil wastewater. *Environ. Sci. Technol.* **2000**, *34* (14), 2990−2996.

(14) Belkacem, M.; Hadjiev, D.; Aurelle, Y. A model for calculating the steady-state flux of organic ultrafiltration membranes for the case of cutting oil emulsions. *Chem. Eng. J.* **1995**, *56*, 27−32.

(15) Viadero, R. C.; Masciola, D. A.; Reed, B. R.; Vaughan, R. L. Two-phase limiting flux in high-shear rotary ultrafiltration of oil-in-water emulsions. *J. Membr. Sci.* **2000**, *175*, 85−96.

(16) Mulder, M. *Basic Principles of Membrane Technology*, 2nd ed.; Kluwer Academic Publishers: Dordrecht, The Netherlands, 2000.

Received for review July 25, 2003. Revised manuscript received January 13, 2004. Accepted June 29, 2004.

ES0348243